Laser Sintered Porous Ti–6Al–4V Implants Stimulate Vertical Bone Growth

Alice Cheng, [1,2]

David J. Cohen, [3]

Adrian Kahn, [4]

Ryan M. Clohessy, [3]

Kaan Sahingur, [3]

Joseph B. Newton, [3]

Sharon L. Hyzy, [3]

Barbara D. Boyan, [1,3,6,*]

Phone 804-828-0190
Email bboyan@vcu.edu

Zvi Schwartz, [3,5]

[1] Wallace H. Coulter Department of Biomedical Engineering, Georgia Institute of Technology and Emory University, Atlanta, GA, USA

[2] Department of Biomedical Engineering, Peking University, Beijing, China

[3] Department of Biomedical Engineering, Virginia Commonwealth University, Richmond, VA, USA

[4] Department of Oral Surgery, University of Tel-Aviv, Tel Aviv, Israel

[5] Department of Periodontics, University of Texas Health Science Center at San Antonio, San Antonio, TX, USA

[6] School of Engineering, Virginia Commonwealth University, 601 West Main Street, Richmond, VA, 23284 USA

Abstract

The objective of this study was to examine the ability of 3D implants with trabecular-bone-inspired ~~that possess~~ porosity ~~inspired by trabecular bone~~ and ~~surface~~ micro-/nano-rough~~ness,~~ surfaces to enhance vertical bone ingrowth. Porous Ti–6Al–4V constructs were fabricated via laser-sintering and processed to obtain micro-/nano-rough surfaces. Male and female human osteoblasts were seeded on constructs to analyze cell morphology and response. Implants were then placed on rat calvaria for 10 weeks to assess vertical bone ingrowth, mechanical stability and osseointegration. All osteoblasts showed higher levels of osteocalcin, osteoprotegerin, vascular endothelial growth factor and bone morphogenetic protein 2 on porous constructs compared to solid laser-sintered controls. Porous implants placed *in vivo* resulted in an average of 3.1 ± 0.6 mm^3 vertical bone growth and osseointegration within implant pores and had significantly higher pull-out strength values than solid implants. New bone formation and pull-out strength was not improved with the addition of demineralized bone matrix putty. Scanning electron images and histological results corroborated vertical bone growth. This study indicates that Ti–6Al–4V implants fabricated by additive manufacturing to have porosity based on trabecular bone and post-build processing to have micro-/nano-surface roughness can support vertical bone growth *in vivo,* and suggests that these implants may be used clinically to increase osseointegration in challenging patient cases.

Keywords

Biomaterials
Gender differences
Guided tissue regeneration
Osteoblasts
Osseointegration
Surface properties

Associate Editor Sean S. Kohles oversaw the review of this article.

Alice Cheng and David J. Cohen contributed equally to this work.

Introduction

Dental implant success remains a challenge for compromised patients such as the elderly, smokers, diabetics and patients undergoing irradiation therapy of the head and neck.[17] Implants with porosity are now being introduced as a way to enhance bone formation in compromised patients.[2] Histological studies in the rabbit have also indicated blood vessel formation in concavities of implants, suggesting that porosity may also enhance vascularization.[21]

Titanium and its alloys are still the preferred materials for bone interfacing implants based on their ability to osseointegrate, as well as their corrosion resistance and mechanical properties.[8,11] Although tantalum-coated porous implants have been introduced into the market, they have shown only comparable but not superior performance to solid implants.[15] In addition, these and other porous implants made using traditional manufacturing techniques cannot be manufactured in one piece, requiring additional processing.

Selective laser sintering (SLS) is a form of additive manufacturing that is able to create high resolution, patient-specific titanium–aluminum–vanadium (Ti–6Al–4V) constructs and bone-interfacing implants in one step. By increasing porosity, compressive moduli of the constructs decreased to better mimic the natural modulus of bone.[5] Previous studies have shown that human osteoblasts exhibit higher expression of factors favoring osteoblastic differentiation and maturation, including osteocalcin, vascular endothelial growth factor (VEGF) and bone morphogenetic proteins (BMPs) when cultured on 3D porous constructs compared to 2D solid constructs.[5,6] In addition, animal studies have indicated that SLS Ti–6Al–4V implants support vertical bone growth when equally spaced through-pores are included.[7,13]

These promising results suggested that porosity is an important design element for stimulating vertical bone formation needed to anchor implants on the surface of compromised bone. However, *in vivo*, bone porosity is not strictly linear. Therefore the present study examined the hypothesis that porosity created using a bone biomimetic would stimulate osteoblast differentiation *in vitro* and promote implant osseointegration *in vivo*. To test this hypothesis, we used SLS technology to generate Ti–6Al–4V constructs with porosity based on human trabecular bone and hierarchical micro-/nano-surface roughness. We examined human osteoblast response to these constructs, then assessed their effectiveness at supporting vertical bone growth in a rat cranial onlay model with and without the use of demineralized bone matrix putty to stimulate osteogenesis.

Materials and Methods

Materials Manufacturing

All constructs were fabricated and characterized as described previously.[5,6] Briefly, constructs were laser-sintered from Ti–6Al–4V powder using a "medium porosity, high resolution" template based on human trabecular bone (563 ± 2 μm average porosity). The porosity was determined using a microCT scan of human femoral head trabecular bone that was overlaid on itself multiple times. Post-build processing involved grit blasting exposed surfaces with calcium phosphate particles under a proprietary commercial protocol (AB Dental, Ashdod, Israel). This was followed by acid etching in 0.3 N nitric acid and pickling in a 1:1 solution of NaOH and H_2O_2 to obtain micro-/nano-surface roughness on all surfaces. Implants for histology had a solid or porous base 3.5 mm in width and 5 mm in length between two 0.75 mm solid supports on either side, and were 2 mm in height (Fig. 1a). Implants for mechanical testing included an additional arch 2.5 mm in height connected to the solid side supports (Fig. 1b). Constructs for cell studies were manufactured with the same porosity as implants, but were 15 mm in diameter and 5 mm in height (including a 1 mm solid base) to fit snugly within wells of a 24-well plate.

Figure 1

Implants for histology (a) and mechanical testing (b). Blue indicates solid side support and arch for mechanical testing; red indicates either solid or trabecular porosity based on experimental group. SEM images of solid (left) and 3D porous (right) implants showing macro, micro and nano-surface topography (c); implant surface chemistry (d); and contact angle of solid implant surfaces (e).

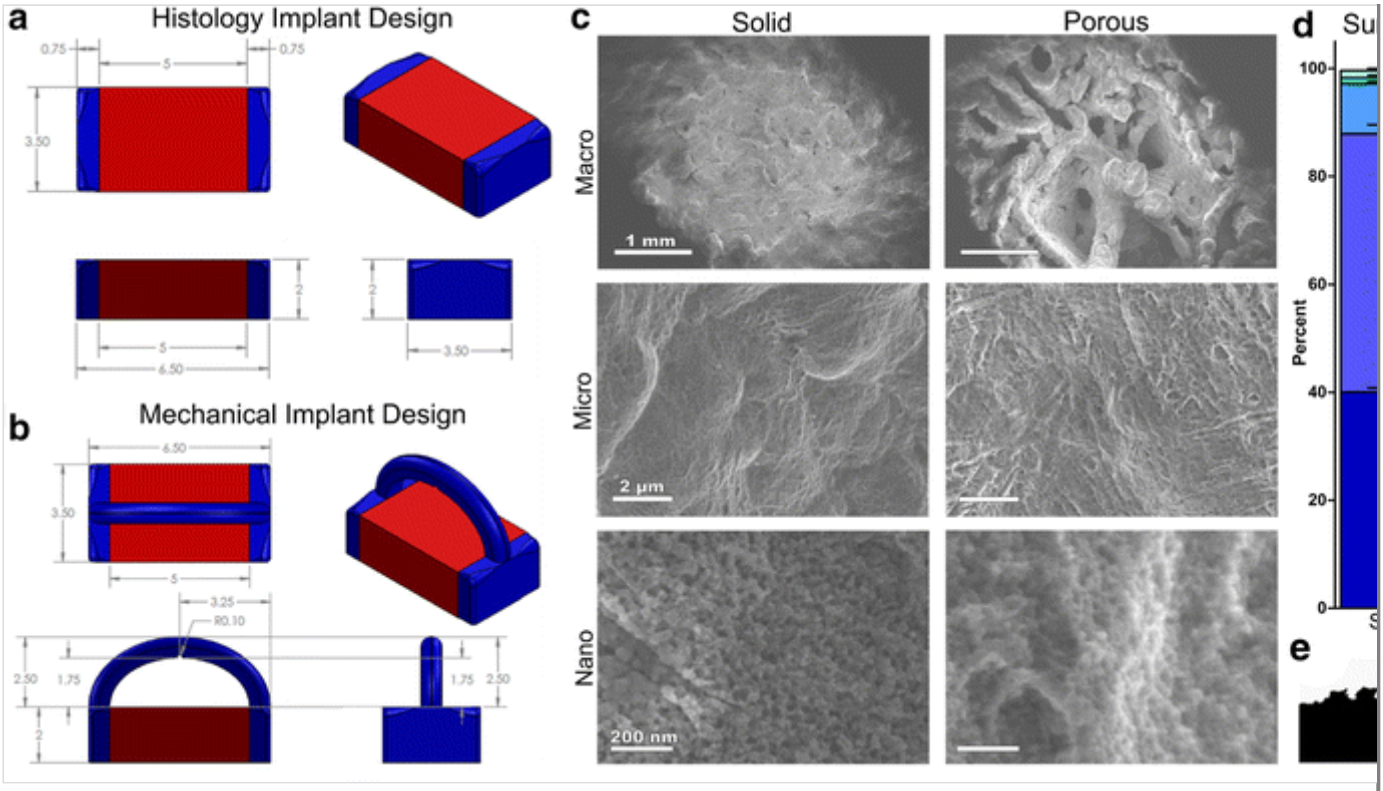

Material Characterization

Material characterization was performed for implants only; material characterization of constructs used for *in vitro* studies was previously performed and published.[5] Surface chemistry was determined using X-ray photoelectron spectroscopy (XPS, ESCAlab 250, ThermoFisher, Waltham, MA). Aluminum clips were sonicated in acetone for 10 min prior to use in securing samples. Analysis was conducted using an XR5 gun, 500 μm spot size, 20 ms dwelling time and 1 eV energy step size. Six spots were analyzed per implant, with two implants per group (n = 12).

Sessile drop contact angle was performed on solid implants (Ramé-Hart, Succasunna, NJ) to evaluate wettability of implant surfaces. A 1μL drop of distilled water was placed on implants. The average of left and right contact angles of the drop were calculated every 5 s for 20 s using DROPImage software (Ramé-Hart). Three drops were placed per implant for two implants (n = 6).

Implants were imaged using scanning electron microscopy (SEM, Zeiss AURIGA, Zeiss, Oberkochen, Germany). Imaging was conducted in Inlens mode with an accelerating voltage of 4 kV and working distance of 4–6 mm.

Micro-computed tomography (microCT, Skyscan 1173, Bruker, Kontich, Belgium) was used to analyze implant porosity. Implants were scanned at a resolution of

1120x1120 pixels, using a brass 0.25 mm filter with a voltage of 120 kV, current of 60 μA, image pixel size of 20.13 μm, exposure time of 300 ms and rotation step of 0.2 degrees. A standard Feldkamp reconstruction was performed with a Gaussian smoothing kernel of zero and a beam hardening correction of 20% using NRecon software version 1.6.9.17 (Bruker) and analyzed in CT-Analyser version 1.14.4.1 (Bruker). Constructs were binarized and total porosity was calculated within a fixed VOI averaged over $n = 3$ constructs.

Cell Response

Normal human osteoblasts (NHOst) (Lonza, Walkersville, MD) from two different Caucasian donors were used in the study: a 20yo male donor (#27625) and a 32yo female donor (#28014). Cells were plated on clear tissue culture polystyrene (TCPS) to observe confluence, or on solid or porous constructs at a density of 60,000 cells per well. Each group had $n = 6$ for both male and female cells. Cells were cultivated in Dulbecco's modified Eagle medium (DMEM) supplemented with 10% fetal bovine serum (FBS) and 1% penicillin/streptomycin, and medium was replaced 24 h after plating. At confluence according to TCPS, medium was exchanged. Cells were harvested 24 h after confluence by rinsing twice with phosphate buffered saline (1xPBS). Media were analyzed for osteocalcin, osteoprotegerin (OPG), vascular endothelial growth factor (VEGF) and bone morphogenetic protein 2 (BMP2), and these were normalized to DNA content. Whole cell lysates were used to analyze DNA content, alkaline phosphatase activity (ALP) and total protein content. ALP was normalized to total protein content. Experiments were repeated to ensure validity of results, and representative results are published.

For imaging, cells were fixed in 4% paraformaldehyde, then dehydrated in a series of increasing ethanol solutions and hexamethyldisilazane (HMDS) as reported previously.[6] Samples were sputtered with platinum prior to SEM imaging.

Cranial Bone Onlay Model

Methods for the cranial bone onlay model and subsequent characterization were adapted from a previously published study.[7] Eight-week old 250–300 g male athymic nude rats (Hsd:RH-Foxn1^{rnu}, Harlan Laboratories, Indianapolis, IN) were used to evaluate effects of human bone graft substitute on implant osseointegration without rejection. Rats were anesthetized with 1.2 L/min of flowing isoflurane and 0.2% oxygen. Hair was removed from the head with depilatory cream. A 2 cm incision was made on the calvarium to the right of the sagittal suture, and the

periosteum was elevated. A dental burr was used to perforate the calvarial bone 10–15 times at the site of implant placement in order access the marrow space and allow for stem cell infiltration.[22] Three experimental groups were used in this study, with animals randomized for each group. For Solid and Porous groups, a solid or porous implant was placed on top of the calvarial bone. For the Porous + DBX group, human demineralized bone matrix putty (DBX, Musculoskeletal Transplant Foundation, Edison, NJ) was placed on the bottom surface of implants in contact with the calvaria as an osteoinductive material for bone growth into implant pores. Each group (Solid, Porous, and Porous + DBX) had n = 8 rats for histology and an additional n = 8 rats for mechanical testing. Implants were secured to the calvarium using a purse-string suture to close the periosteum around the implant, and the skin was sutured closed. Rats were housed in single cages with access to food and water, and weighed at least once a week to ensure healthy recovery. Rats were euthanized at 10 weeks post-surgery. All animal procedures were approved by and carried out in accordance with the Virginia Commonwealth University Institutional Animal Care and Use Committee and reported according to ARRIVE guidelines.

Mechanical Testing

Rat calvaria harvested for mechanical testing were stored overnight at 4 °C without formalin. All samples were tested on the same day so that differences across groups could be compared. The head was loaded into a custom testing device with the implant aligned to the testing machine axis to minimize bending during the test (MTS Insight 30; MTS Corp., Eden Prairie, MN, USA). A stainless steel wire (0.02 in diameter, Malin Co., Cleveland, OH, USA) was threaded through the arch of the implant and pulled at a crosshead speed of 5 mm/min. Axial pull-out strengths and force at failure (N) were recorded.

MicroCT

Rat calvaria harvested for microCT and histology were stored in 10% formalin. MicroCT scans and reconstructions were performed as described above. After binarization, a volume of interest (VOI) was applied along the 5 mm porous or solid length of implants (not including the solid sides) and extending 500 μm in the z-direction. The VOI was shrink-wrapped around the implant and then dilated to include an 80 μm border to minimize error from image scattering. The implant was subtracted from the VOI, and the remaining bone in contact with the void space within a 20 μm perimeter where the implant had been subtracted was shrink-wrapped, thresholded and quantified. Basal bone-implant contact was calculated by

taking the volume of bone measured in the VOI divided by the volume of implant measured in the VOI. To calculate total bone volume in porous implants, bone was binarized and quantified after thresholding from the implant. To calculate bone volume as a percentage of total porous implant volume, the total bone volume was divided by the implant porous volume within the VOI.

Histology

Calvaria were prepared for histological sectioning by setting in poly (methyl methacrylate) (Histion, LLC, Everett, WA). Sections were stained using Stevenel's Blue to show bone in purple and connective tissue in blue.[16] The Zen 2012 Blue Edition software with an AxioCam MRc5 camera and Axio Observer Z.1 microscope (Carl Zeiss Microscopy, Oberkochen, Germany) was used to image slides using an N-Achroplan 10×/0.25 Ph1 M27 objective. Calculation of bone area below the implant was performed as a modification of previously published analysis method for expected bone-to-implant contact (BIC).[24] Briefly, bone area was quantified 0.5 mm below a straight line connecting the outer boundaries of the implant. Bone ingrowth into the implants was calculated by dividing the total area of bone within the implant by the total porous area of the implant. The porous area was calculated between the upper and lower boundaries of each implant. The total area of the bone in the implant was then calculated by finding the area of the bone present within the boundaries of the implant.

Statistical Analysis

An unpaired *t* test was performed to compare differences between two groups. A one-way analysis of variance (ANOVA) was performed to compare across three or more groups, with Bonferroni post hoc analysis to determine significance between individual groups. A $p < 0.05$ indicated statistical significance. All statistical analyses were conducted using GraphPad Prism software (GraphPad, La Jolla, CA).

Results

Material Characterization

SEM images show the macro-, micro- and nano- features produced after surface treatment on both solid and porous implants (Fig. 1c). MicroCT analysis of porous constructs revealed an interconnected porosity of 67 ± 3%. XPS analysis showed that both solid and porous implants possessed oxygen, carbon, titanium, nitrogen and calcium on their surfaces (Fig. 1d). Porous implants additionally had a small

percentage of phosphorous present. Solid implants possessed a contact angle of $47^{o} \pm 17^{o}$ (Fig. 1e).

Cell Response

NHOst cells plated on solid disks (Fig. 2a, top) and porous constructs (Fig. 2a, bottom) showed elongated morphology with extended filopodia. Cells were observed suspended across struts and crevasses on porous constructs. Less cells were observed on porous constructs compared to on solid disks. DNA content was decreased on solid and porous constructs compared to TCPS and solid constructs (Fig. 2b), confirming the morphological observations.

Figure 2

NHOst cells on solid (top) and 3D porous (bottom) constructs with increasing magnification from left to right (a); DNA content (b); alkaline phosphatase specific activity (c); osteocalcin (d); osteoprotegerin (e); vascular endothelial growth factor (f); and bone morphogenetic protein (g) of male and female NHOst cells on 2D and 3D porous constructs. 1 way ANOVA with Bonferroni post hoc test, $p < 0.05$, *vs. TCPS ^ vs. 2D. Unpaired t test, $p < 0.05$, # vs. Female. Scale bars represent 100 μm.

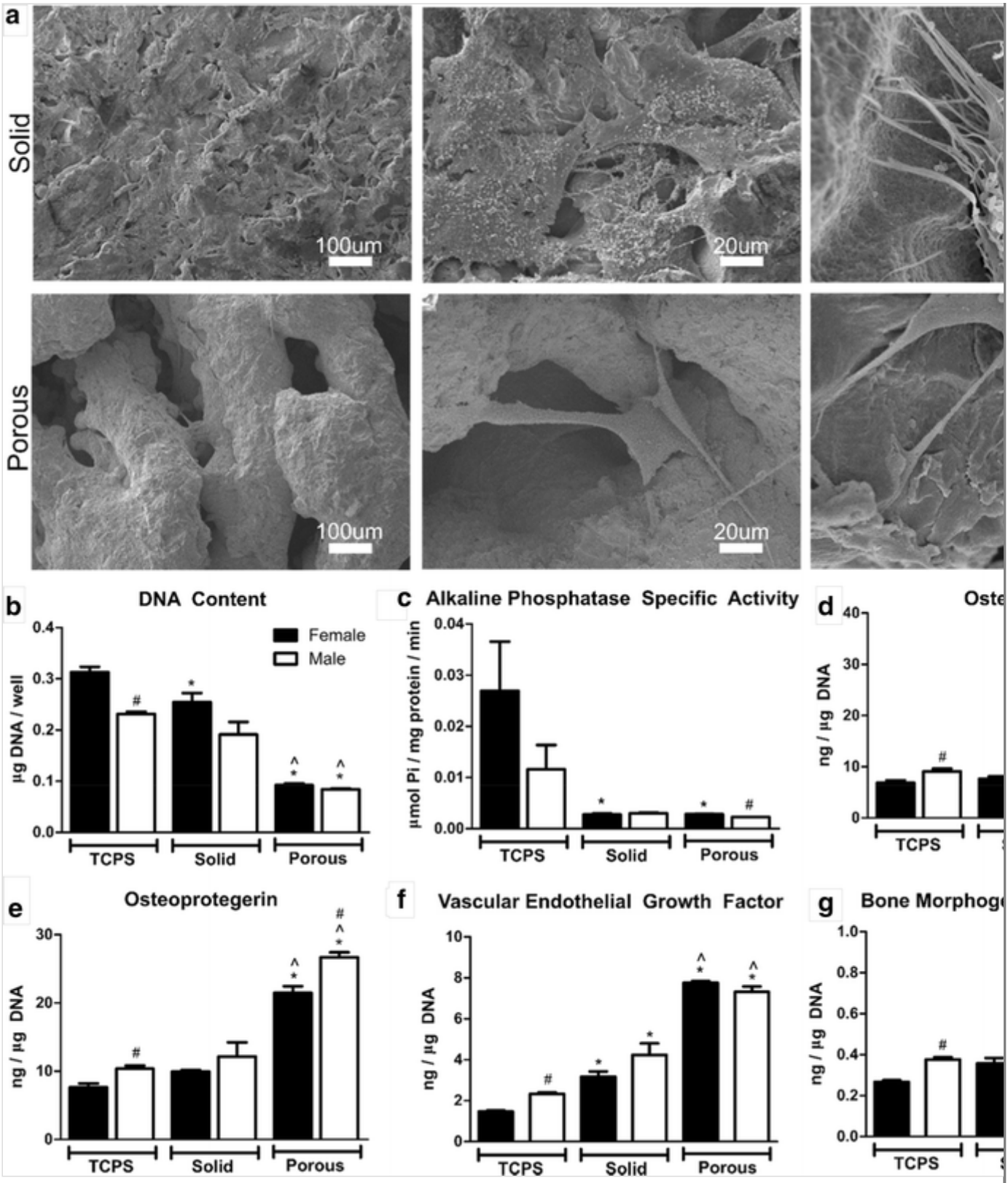

Osteoblast differentiation was sensitive to implant porosity. Alkaline phosphatase specific activity was significantly lower on solid and porous constructs compared to TCPS for female NHOst cells only (Fig. 2c). In contrast, osteocalcin was significantly increased on porous constructs compared to TCPS and solid disks for both female and male NHOsts (Fig. 2d). Moreover, male NHOsts exhibited

significantly higher levels of osteocalcin than female NHOsts on TCPS and solid disks. Osteoprotegerin was significantly increased on porous constructs compared to TCPS and solid disks for both female and male NHOsts (Fig. 2e). Male NHOsts had significantly higher levels of osteoprotegerin on TCPS and porous constructs compared to female NHOsts. Vascular endothelial growth factor (VEGF) was significantly increased on solid disks and porous constructs compared to TCPS, and porous constructs compared to solid disks for both male and female NHOsts (Fig. 2f). VEGF was higher for male NHOsts on TCPS compared to female NHOsts. Bone morphogenetic protein 2 (BMP2) was significantly increased on porous constructs compared to TCPS and solid disks for both male and female NHOsts, and was increased for male NHOsts on TCPS compared to female NHOsts (Fig. 2g).

MicroCT Analysis

We used a calvarial onlay implantation procedure for this study, which allowed us to correlate bone-to-implant contact measured histologically with mechanical strength (Fig. 3a). One rat died the first week after surgery from the Solid group; results are reported for $n = 7$ rats for the Solid group and $n = 8$ rats for Porous and Porous + DBX groups. MicroCT images contrasted bone growth below Solid implants (Fig. 3b) with vertical bone growth into Porous (Fig. 3c) or Porous + DBX implants (Fig. 3d). These qualitative observations were corroborated by quantitative analysis. BIC across the base of the implant was higher for Porous + DBX implants compared to Solid implants, but was not significantly different between Porous and Porous + DBX groups (Fig. 3e). Solid implant BIC was 20% ± 3.6 for Solid implants, 25 ± 1.4% for Porous implants and 33 ± 2.7% for Porous + DBX implants. Bone growth expressed as total volume (Fig. 3f) or percentage of porous construct void volume (Fig. 3g) was also not significantly different for porous implants with or without DBX. Total bone volume within pores was 3.1 ± 0.60 mm^3 for Porous and 2.5 ± 0.18 mm^3 for Porous + DBX implants. This constituted 6.2 ± 0.76% of the porous volume of implants for Porous implants, and 4.8 ± 0.46% of the porous volume for Porous + DBX implants.

Figure 3

Surgery schematic. An initial incision was made and the periosteum was lifted. 15–20 pilot holes were drilled to allow for stem cell infiltration before implant placement. Implants were placed atop the calvarial bone and tightly secured by a purse-string suture of the periosteum around the implant. Animals were harvested after 10 weeks for pull-out testing or microCT followed by histology (a). MicroCT cross-sectional

images of 2D (~~a~~b), 3D (~~b~~c) and 3D with DBX implants (~~c~~d) on rat calvaria 10 weeks after implantation. Bone to implant contact (~~d~~e), volume of bone growth into implant pores (~~e~~f) and percent volume of bone growth into implant pores (~~f~~g) as analyzed by microCT analysis. 1 way ANOVA with Bonferroni post hoc test, $p < 0.05$, *vs. 2D. Unpaired t test, $p < 0.05$. No significance.

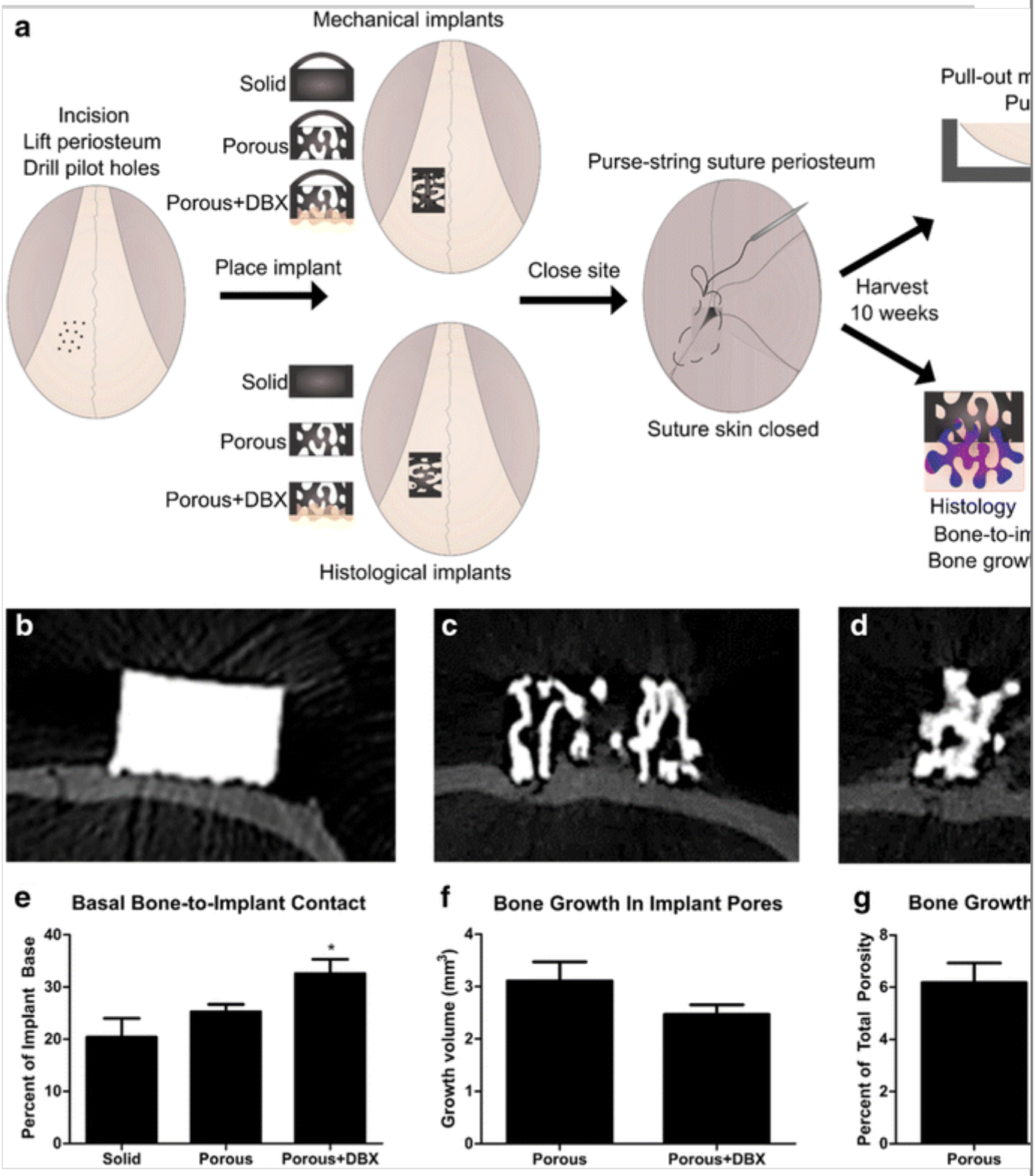

AQ1

Mechanical Testing

Pull-out values of implants were significantly higher for Porous and Porous + DBX compared to Solid implants, but the use of DBX did not contribute to a significant increase in pull-out force for porous implants (Fig. 4a). Optical (Fig. 4b) and SEM (Fig. 4c) images of rat calvaria after pull-out testing show a relatively smooth surface for calvaria with solid implants, while calvaria with porous implants showed rough locations of bone growth and breaking points during testing. Optical (Fig. 4d) and SEM (Fig. 4e) images of implants after mechanical testing show limited periosteum and bone on solid implants, while large portions of bone and periosteum were integrated inside pores of porous implants.

Figure 4

Pull-out force 10 weeks after implantation (a), with corresponding optical (b, d) and SEM (b, e) images of calvaria (b, c) and implant (d, e) after mechanical testing.

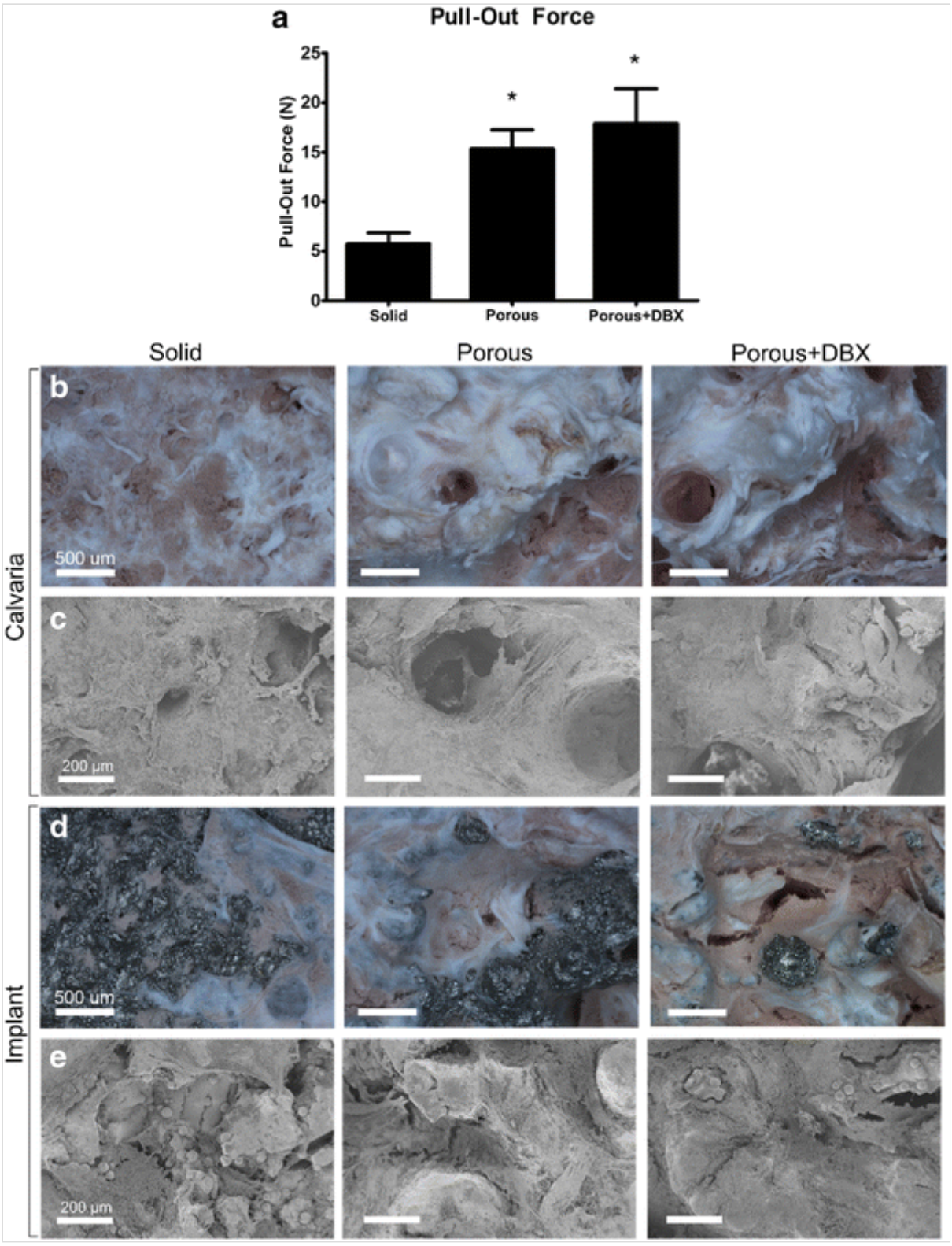

Histology

Histological cross-sections of solid implants (Fig. 5a) showed BIC occurring near the middle of implants. In contrast, Porous (Fig. 5b) and Porous + DBX implants (Fig. 5c) showed bone ingrowth into pores and all along the base of the implant. Bone area calculated 0.5 mm below the implant base was 2.97 ± 0.23, 2.52 ± 0.14

and 2.61 ± 0.14 mm^2 for Solid, Porous and Porous + DBX implants, respectively (Table 1). These values were not significantly different among implant groups (Fig. 5d). New bone growth into porous implants was 1.62 ± 0.21 mm^2 for Porous implants and 1.52 ± 0.34 mm^2 for Porous + DBX implants, which were not significantly different from each other (Table 1). This constituted 21% ± 2.4% of the area for Porous implants and 20 ± 4.8% for Porous + DBX implants (Fig. 5e). Porous + DBX had an additional 1.29 ± 0.27 mm^2 of DBX remaining within the implant pores, or 16 ± 3.0% of the porous area (Table 1, Fig. 5e).

Figure 5

Histological sections of 2D (a), 3D (b) and 3D with DBX (c) implants 10 weeks after implantation. Bone area 0.5 mm below the implant base (d) and percent growth of bone into implant pores (e) determined from histological analysis (e). Scale bars represent 1 mm.

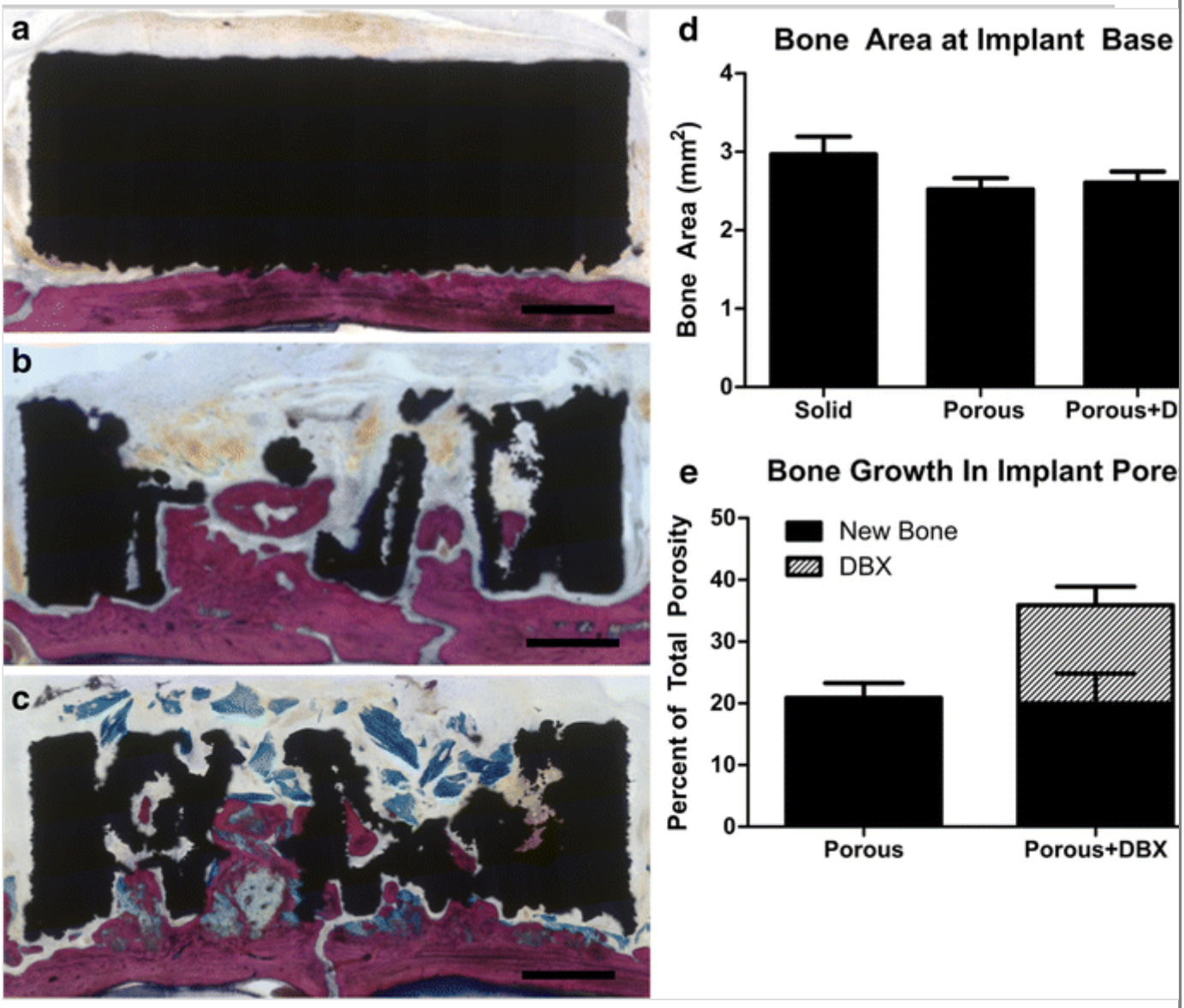

Table 1

Histological analysis of total bone and new bone growth into 3D implants.

	Solid	Porous	Porous + DBX
Histological analysis (average ± SEM)			
Bone 0.5 mm below implant base (mm^2)	2.97 ± 0.23	2.52 ± 0.14	2.61 ± 0.14
New bone (mm^2)	–	1.62 ± 0.21	1.52 ± 0.34
DBX (mm^2)	–	–	1.29 ± 0.27

Discussion

This objective of this study was to examine the influence of a trabecular-inspired porosity manufactured by laser sintering on cell response and bone ingrowth. While there was donor variability for some factors, in general osteoblasts from both donors responded more favorably to porous constructs compared to solid substrates. The effect of a 3D trabecular porosity was also observed *in vivo*, where porous implants were able to support vertical bone growth even without the addition of exogenous factors.

Laser sintering was used to produce constructs for *in vitro* and implants for *in vivo* studies. We use the term “construct” in this text to be inclusive of all previous and potential uses of laser sintering technology, including for tissue regeneration scaffolds. The manufacturing and surface post-processing techniques used in this study have been previously published, and our constructs have comparable surface chemistry, hydrophilicity and multi-scale topography as other manufactured batches.[4–6] We and others have shown previously that surface micro- and nano-roughness, along with surface wettability, enhances markers for osteoblast differentiation and maturation *in vitro*, and osseointegration *in vivo*.[12] We wanted to make sure that we were able to retain the same surface characteristics that enhanced osteoblast response in previous *in vitro* studies.[5] Because our manufacturing techniques remained the same for all materials in this study, we did not additionally characterize material properties for implants. Since all materials were also sintered from the same template, differences in total percent porosity between implants and constructs can be explained by differences in implant geometry and VOI used for microCT analysis.

Our results show the importance of using cells from more than one donor, and both sexes, in determining the effects of biomaterial design on human MSCs. Even

though there were donor-specific differences noted in our study, overall the effect of porosity was to enhance osteoblast differentiation. Studies on sex differences have traditionally focused on gender-specific diseases, but a recent report by collaborators at the National Institutes of Health and the American Academy of Orthopaedic Surgeons has pushed for inclusion of sex differences in musculoskeletal health.[23] Previously, our lab investigated the effect of surface roughness on male and female cells isolated from rats, showing that male cells were more responsive to 1α,25-dihydroxyvitamin D3 on titanium surfaces than female cells.[18] Other studies evaluating biological effects of additively manufactured titanium aggregated the responses of male and female cells from humans for analysis.[14] In this study, only one donor from each sex was examined as a preliminary experiment prior to the animal study. Although we cannot draw strong conclusions on differences in specific protein levels between male and female cells on our materials, both sexes produced more factors for osteoblastic differentiation and maturation on the 3D porous constructs compared to the solid substrates. Because osteoblast response can vary across experimental conditions and with donor age, we suggest that future studies continue to consider sex differences and use multiple donors when evaluating cell response to implant materials.[3,19]

Our results indicate that new bone ingrowth into the pores of the implant is correlated positively with mechanical strength of the interface. Pull-out force values supported microCT results, indicating enhanced osseointegration for porous compared to solid implants, regardless of DBX use. Optical and electron images showing bone nodules on calvaria and new bone in implant pores, combined with microCT observations and pull-out force values, indicate that bone was strongly osseointegrated within surfaces of porous implants and that failure at the base of the implant contributed more to pull-out force. This also indicates that new bone quality was similar for porous implants with or without DBX, and superior to that of solid implants. Bone area at the implant base was calculated as a proxy for bone to implant contact for histology samples. Although histology processing contributed to irregularities in visualizing direct bone to implant contact, the bone ingrowth and bone underneath the implants corroborate the quality of osseointegration shown by microCT and electron image analyses.

Surprisingly, the use of DBX did not significantly enhance mechanical pull-out testing force or total vertical bone volume growth into porous implants. A review on ridge augmentation procedures suggests that implant success in augmented areas is a function of the residual bone and less a function of the grafted bone.[1] Our results corroborate this finding. Although 16% of DBX still remained in implants

after 10 weeks, this had no discernable effect on the mechanical functionality of implants. This also points to the importance of supporting natural bone growth, in contrast to using large bone block substitutes. Previous work by our lab also showed DBX remaining when using the same cranial bone onlay model.[7] A study of three different types of demineralized bone matrix (DBM) in rat spines showed varying amounts of residual DBM after 8 weeks, indicating that the formatting of DBM is also an important factor to consider.[20]

Because our study ended at 10 weeks, it is possible that bone would continue to form over longer time periods. A previous dental implant study in humans without the use of bone substitutes showed that there was still coronal bone formation occurring even at 9 months after implant placement with a non-resorbable membrane.[22] In a previous study of laser sintered constructs using the same cranial bone onlay model, we observed significant differences between groups after 10 weeks.[7] Although longer term and larger animal studies are necessary for evaluating implant survival, our results suggest that porous implants can be successfully placed in areas with insufficient bone to induce vertical bone regeneration.

Most clinical procedures for implant placement in patients with insufficient bone volume still require the use of a bone substitute or sophisticated surgical techniques to achieve vertical bone growth.[9] Our study suggests that bone-interfacing, laser sintered implants with a natural inspired porosity may be better able to leverage the regenerative potential of patients, which may be useful for challenging clinical cases. Laser sintered trabeculae-inspired porosity implants may also achieve superior long-term clinical outcomes over traditional solid implants in compromised patients. The ability to customize implant size and increase bone ingrowth also counteracts improper implant planning and bone resorption, factors that contribute to implant fracture.[10]

It should be noted that both solid and porous Ti–6Al–4V implants used in this study had microscale and nanoscale surface texture, which has been shown previously to enhance osteogenic differentiation of mesenchymal stem cells *in vitro* and osseointegration *in vivo*.[4,13] Thus, the enhanced bone-to-implant contact and mechanical stability noted with porous implants is a reflection of their increased surface area resulting from their porosity, and not due to differences in surface processing alone. A trabecular porosity may optimize growth factor accumulation and signaling between osteoblasts and mesenchymal stem cells near the implant site, inducing bone growth into the implant pores.

Conclusion

Laser sintering is a scalable and consistent manufacturing technique that can be used to produce bone-interfacing Ti–6Al–4V implants with human trabecular bone-inspired porosity. The combination of a unique manufacturing method with heterogeneous porosity and surface post-processing yield implants with the ability to not only osseointegrate, but also promote vertical bone growth in the rat calvaria. The addition of DBX did enhance the amount of new bone formed, suggesting that proper implant design alone can achieve better clinical results. Thus, future implants with personalized geometry and porosity can be more accessible and functional than current options of treatment.

Acknowledgments

Research reported in this publication was supported by the National Institute of Arthritis and Musculoskeletal and Skin Diseases of the National Institutes of Health under Award Number AR052102. The content is solely the responsibility of the authors and does not necessarily represent the official views of the National Institutes of Health. The authors would like to thank AB Dental for generously donating materials for this study. AC was supported by a National Science Foundation Graduate Research Fellowship. BDB is a paid consultant for Titan Spine LLC and an unpaid consultant for Institut Straumann AG. ZS is a paid consultant for AB Dental.

References

1. Aghaloo, T. L., and P. K. Moy. Which hard tissue augmentation techniques are the most successful in furnishing bony support for implant placement? *Int. J. Oral Maxillofac. Implant.* 22(Suppl):49–70, 2007.

2. Brauner, E., G. Guarino, S. Jamshir, P. Papi, V. Valentini, V. Pompa, and G. Pompa. Evaluation of highly porous dental implants in postablative oral and maxillofacial cancer patients: a prospective pilot clinical case series report. *Implant Dent.* 24(5):631–637, 2015.

3. Chavassieux, P. M., C. Chenu, A. Valentin-Opran, B. Merle, P. D. Delmas, P. J. Meunier, D. J. Hartmann, and S. Saez. Influence of experimental conditions on osteoblast activity in human primary bone cell cultures. *J. Bone Miner. Res.* 5(4):337–343, 1990.

4. Cheng, A., D. J. Cohen, B. D. Boyan, and Z. Schwartz. Laser sintered constructs with bio-inspired porosity and surface micro/nano roughness enhance mesenchymal stem cell differentiation and matrix mineralization in vitro. *Calcif. Tissue Int.* 99:625–637, 2016.

5. Cheng, A., A. Humayun, B. D. Boyan, and Z. Schwartz. Enhanced osteoblast response to porosity and resolution of additively manufactured Ti-6Al-4V constructs with trabeculae-inspired porosity. *3D Print. Addit. Manuf.* 3(1):10–21, 2016.

6. Cheng, A., A. Humayun, D. J. Cohen, B. D. Boyan, and Z. Schwartz. Additively manufactured 3D porous Ti-6Al-4V constructs mimic trabecular bone structure and regulate osteoblast proliferation, differentiation and local factor production in a porosity and surface roughness dependent manner. *Biofabrication* 6(4):045007, 2014.

7. Cohen, D. J., A. Cheng, A. Kahn, M. Aviram, A. J. Whitehead, S. L. Hyzy, R. M. Clohessy, B. D. Boyan, and Z. Schwartz. Novel osteogenic Ti-6Al-4V device for restoration of dental function In patients with large bone deficiencies: design, development and implementation. *Sci. Rep.* 6:20493, 2016.

8. Elias, C. N., D. J. Fernandes, C. R. S. Resende, and J. Roestel. Mechanical properties, surface morphology and stability of a modified commercially pure high strength titanium alloy for dental implants. *Dent. Mater.* 31(2):e1–e13, 2015.

9. Esposito, M., M. G. Grusovin, P. Felice, G. Karatzopoulos, H. V. Worthington, and P. Coulthard. The efficacy of horizontal and vertical bone augmentation procedures for dental implants—a Cochrane systematic review. *Eur J Oral Implantol* 2(3):167–184, 2009.

10. Gealh, W. C., V. Mazzo, F. Barbi, and E. T. Camarini. Osseointegrated implant fracture: causes and treatment. *J Oral Implantol* 37(4):499–503, 2011.

11. Geetha, M., A. K. Singh, R. Asokamani, and A. K. Gogia. Ti based biomaterials, the ultimate choice for orthopaedic implants—A review. *Prog. Mater. Sci.* 54(3):397–425, 2009.

12. Gittens, R. A., L. Scheideler, F. Rupp, S. L. Hyzy, J. Geis-Gerstorfer, Z. Schwartz, and B. D. Boyan. A review on the wettability of dental implant surfaces II: biological and clinical aspects. *Acta Biomater.* 10(7):2907–2918, 2014.

13. Hyzy, S. L., A. Cheng, D. J. Cohen, G. Yatzkaier, A. J. Whitehead, R. M. Clohessy, R. A. Gittens, B. D. Boyan, and Z. Schwartz. Novel hydrophilic nanostructured microtexture on direct metal laser sintered Ti-6Al-4V surfaces enhances osteoblast response *in vitro* and osseointegration in a rabbit model. *J. Biomed. Mater. Res. A* 104(8):2086–2098, 2016.

14. Jonitz-Heincke, A., J. Wieding, C. Schulze, D. Hansmann, and R. Bader. Comparative analysis of the oxygen supply and viability of human osteoblasts in three-dimensional titanium scaffolds produced by laser-beam or electron-beam melting. *Materials* 6(11):5398–5409, 2013.

15. Kim, D. G., S. S. Huja, B. C. Tee, P. E. Larsen, K. S. Kennedy, H. H. Chien, J. W. Lee, and H. B. Wen. Bone ingrowth and initial stability of titanium and porous tantalum dental implants: a pilot canine study. *Implant Dent.* 22(4):399–405, 2013.

16. Maniatopoulos, C., A. Rodriguez, D. A. Deporter, and A. H. Melcher. An improved method for preparing histological sections of metallic implants. *Int. J. Oral Maxillofac. Implants* 1(1):31–37, 1986.

17. Moy, P. K., D. Medina, V. Shetty, and T. L. Aghaloo. Dental implant failure rates and associated risk factors. *Int. J. Oral Maxillofac. Implant.* 20(4):569–577, 2005.

18. Olivares-Navarrete, R., S. L. Hyzy, B. D. Boyan, Z. Schwartz. Regulation of osteoblast differentiation by acid-etched and/or grit-blasted titanium substrate topography Is enhanced by 1,25(OH)2D3 in a sex-dependent manner. *BioMed Res. Intl*. 2015, 2015. Article ID 365014.

19. Olivares-Navarrete, R., A. L. Raines, S. L. Hyzy, J. H. Park, D. L. Hutton, D. L. Cochran, B. D. Boyan, and Z. Schwartz. Osteoblast maturation and new bone formation in response to titanium implant surface features are reduced with age. *J. Bone Miner. Res.* 27(8):1773–1783, 2012.

20. Peterson, B., P. G. Whang, R. Iglesias, J. C. Wang, and J. R. Lieberman. Osteoinductivity of commercially available demineralized bone matrix. Preparations in a spine fusion model. *J. Bone Joint Surg. Am.* 86(10):2243–2250, 2004.

21. Scarano, A., V. Perrotti, L. Artese, M. Degidi, D. Degidi, A. Piattelli, and G. Iezzi. Blood vessels are concentrated within the implant surface concavities: a histologic study in rabbit tibia. *Odontology* 102(2):259–266, 2013.

22. Simion, M., P. Trisi, and A. Piattelli. Vertical ridge augmentation using a membrane technique associated with osseointegrated implants. *Int. J. Periodontics Restor. Dent.* 14(6):496–511, 1994.

23. Tosi, L. L., B. D. Boyan, and A. L. Boskey. Does sex matter in musculoskeletal health? A workshop report. *Orthop. Clin. N. Am.* 37(4):523–529, 2006.

24. Trisi, P., R. Lazzara, W. Rao, and A. Rebaudi. Bone-implant contact and bone quality: evaluation of expected and actual bone contact on machined and osseotite implant surfaces. *Int. J. Periodontics Restor. Dent.* 22(6):535–545, 2002.